

## REDUCED ORDER MODELS FOR BLADE-TO-BLADE DAMPING VARIABILITY IN MISTUNED BLISKS

**Anish G. S. Joshi**

Vibrations and Acoustics Laboratory  
Department of Mechanical Engineering  
University of Michigan  
Ann Arbor, Michigan 48109  
Email: ajozi@umich.edu

**Bogdan I. Epureanu\***

Vibrations and Acoustics Laboratory  
Department of Mechanical Engineering  
University of Michigan  
Ann Arbor, Michigan 48109  
Email: epureanu@umich.edu

### ABSTRACT

*A novel reduced order modeling methodology to capture blade-to-blade variability in damping in blisks is presented. This new approach generalizes the concept of component mode mistuning (CMM) which was developed to capture stiffness and mass mistuning (and did not include variability in damping amongst the blades). This work focuses on modeling large variability in damping. Such variability is significant in many applications, and particularly important for modeling damping coatings. The damping in each of the blades is assumed to be structural at the blade level. However, variability in the damping coefficients of the blades means that the damping is not structural at the system (entire blisk) level. Similar to the CMM based studies, structural damping is used to capture the damping effects due to the mechanical energy dissipation caused by internal friction within the blade material. The steady state harmonic responses of the blades are obtained using the novel reduced order modeling methodology, and are validated by comparison with simulation results obtained using a full order model in ANSYS. The effects of damping mistuning are studied statistically through Monte-Carlo simulations. For this purpose, the blisk model is subjected to multiple travelling wave excitations. The uncertainty in the various mechanisms responsible for dissipation of energy and the uncontrollability of these dissipation mechanisms makes it difficult to assign a reliable value for the loss factor of each blade. Hence large variations (up to  $\pm 80\%$ ) in the structural damping coefficients of the blades are simulated.*

### INTRODUCTION

Ideally, blisks are tuned, i.e. they have cyclic symmetry, which allows for the analysis on the entire blisks to be carried out at a sector level. However, any changes in the structural properties of one or more sectors of a tuned blisk destroy the cyclic symmetry leading to a mistuned system. Due to the destruction of cyclic symmetry, the dynamic response of a blisk can change not only quantitatively, but also qualitatively when compared to the response of a tuned blisk. Blade-to-blade variations in the structural properties of a blisk can result from a variety of reasons. For example manufacturing processes, working conditions and changes in the material properties can cause mistuning. In general, mistuning can occur because of changes in a number of structural properties. In this paper, the focus is primarily on the effects of blade-to-blade variability in damping. Intuitively, a component having lower damping is expected to have higher stress magnitudes compared to a component having higher damping. This is true when all blades vibrate almost independently of each other. Such cases occur for example when the disk has a large thickness, so that vibrations of the disk can be neglected [1]. However, if the disk is thin, the disk modes can interact with the blade modes. This means that the disk surface between adjacent blades can contribute significantly to the overall blade motion. Thus, the motion of one blade can affect the motion of the adjacent blades. This phenomenon has already been observed [2-5]. In particular, the effect of one blade on its neighbors may be different from blade to blade if there is variability in the damping in the blades.

---

\*Address all correspondence to this author.

Although mistuning has beneficial effects in controlling blade flutter boundaries [6–9], it has disadvantageous effects on forced resonant vibration. Mistuning can lead to wide divergences in the peak dynamic stresses from blade to blade, which may be very high when compared to the peak stresses in a tuned system. Hence, it is important to study the effects of mistuning on a system by observing the changes in the steady state resonant frequency response. Various studies have shown that variations of the stiffness from blade to blade leads to shifting and splitting of the resonant frequencies of the blades [10–20]. Theoretical and computational studies have shown that similar effects occur due to variation in frictional damping and viscous damping [6,21,22]. In reality, in a blisk, energy is dissipated by a combination of mechanisms such as material damping, Coulomb friction at the interfaces between sectors, and aerodynamic damping. It is difficult to model the damping by including every mechanism involved. Hence, different damping mechanisms have been studied separately. In the case of blisks, frictional damping is mainly at the disk-blade interface and has been modeled as Coulomb damping. Berthillier *et al.* [23] and Griffin and Sinha [24] have analyzed the effects of dry friction dampers on the forced response of blisks. Wei and Pierre [25] and Muszynska *et al.* [6] have also investigated the dynamic response of cyclic structures with friction damping. In another study, Yoo *et al.* [26] have used a lumped parameter model using coupled pendulum systems to identify the effects of coupled stiffness, mass and damping mistuning. There has also been an attempt to develop reduced order models (ROMs), by modeling the blades as cantilever beams [27, 28] with structural damping [27]. Other examples of the use of structural damping include a receptance model discussed by Ewins [29]. Also, Afolabi [30] has considered variations in the structural damping in the formulation of the complex stiffness matrix. In all these studies, lumped parameter models were used. Petrov [31] used a large scale FEM to develop a method for calculating the nonlinear forced response of bladed disks fitted with friction dampers of various types. Also, using large scale FEMs, Elliot *et al.* [5], Petrov [3] and Petrov *et al.* [2, 4] studied friction damping mistuning and its effects on the dynamics response of bladed disks. Studies by Feiner and Griffin [32, 33] proposed the fundamental model of mistuning (FMM) in which the size of the original model is reduced using a sum of selected system modes to represent the mistuned mode shapes. A recent paper by Siewert *et al.* [34] has extended the FMM methodology to include variability in damping in which the mistuning in damping has been characterized at the sector level as variations in the modal damping values of each sector. In another reduced order modeling method developed by Petrov *et al.* [35] the original size of a detailed FEM has been reduced by selecting a certain number of nodal locations for the calculation of the forced response. In this methodology, the mistuning in damping has been introduced at the desired nodal locations in the form of lumped damping elements between the selected

nodes on each blade and ground, and between two nodes on adjacent blades.

Outside the mistuning community, uncertainty in damping has been studied for example by Hart [36] who investigated the sensitivity of the response of a building to uncertainty in damping and by Kareem and Sun [37] who examined the effects of damping uncertainty on the dynamic response of structures. Also, Kareem and Gurley [38] have studied uncertainty with regards to the prediction and estimation of damping.

The goal of this paper is to develop a novel reduced order modeling methodology to capture blade-to-blade variability in damping amongst the blades of integrally bladed rotors (IBRs) and to highlight the statistical effects of damping variability on the steady state resonant frequency response of the blisk. Structural damping is used to model the energy dissipation due to internal friction in individual blades. This damping model has been used before [27, 29, 30, 39] to model the energy dissipation in bladed disks. In this paper, the damping is assumed to be structural at the blade level. Thus, the damping matrix is proportional to the stiffness matrix at the blade level. Due to variation in the blade damping coefficients amongst the blades, the damping at the system (entire blisk) level does not remain structural. The mistuning in damping is characterized by the deviation of the structural damping coefficients of the blades from their average value. The damping mistuning matrix is then approximated as a mistuned cantilevered blade structural damping matrix. Of particular interest is the application of damping coatings. Such coatings are very thin and provide damping which relates closely to their thickness. Small errors in the coating thickness can lead to large relative variations in the damping amongst the blades. Also, due to uncertainty in the various energy dissipation mechanisms and the uncontrollability of these mechanisms, assigning a reliable value for the loss factor for a blade is difficult [21]. Hence, large blade-to-blade variations in the damping coefficients (as high as  $\pm 80\%$ ) of the blades have been considered in this paper. Note that any nonlinearities such as those due to the damping mechanisms in coatings are neglected.

## MODELING APPROACH

In this section, the derivation of novel ROMs to handle blade-to-blade variability in damping is presented. The models generalize the concept of CMM developed by Lim *et al.* [10, 40] which does not include variability in damping.

This section is organized as follows. First, a brief review of reduced order modeling of mistuned blisks for small mistuning as developed by Lim *et al.* [10] is presented. Next, a step by step development of the novel ROMs which handle blade-to-blade variability in damping is presented.

## ROMs of Mistuned Blisks

Lim *et al.* [10] developed ROMs which capture the effects of stiffness and mass mistuning on the dynamic response of blisks. A component-based modeling framework was used by partitioning the system into a tuned blisk component and a virtual mistuning component. A hybrid-interface component mode synthesis method [41–43] was used to combine the two components by treating the tuned system as a free-interface component, and treating the mistuning component as a fixed-interface component. The mistuning component was defined by the differences between the mistuned and tuned mass and stiffness matrices.

The CMM technique is based on the assumption that blade mistuning is small (compared to nominal properties in the modal domain). According to Yang and Griffin [44, 45], when a tuned bladed disk has normal modes closely spaced in a frequency range, a slightly mistuned bladed disk also features closely spaced modes in the same range. Thus, the mistuned normal modes can be expressed as a linear combination of the tuned normal modes. This means that the tuned normal modes outside of the frequency range of interest, or any static modes, can be ignored in modeling a mistuned system with small mistuning. Hence, blade mistuning can be captured by projecting the mistuned matrices onto only the blade portions of the blisk. Also, it is assumed that the blade-alone mode shapes for a tuned and a mistuned blisk are the same. Next, a technique developed by Bladh *et al.* [15] was used to represent the blade-alone mode shapes using tuned modes of a cantilevered blade fixed at the disk-blade interface. The stiffness mistuning matrices are then projected onto the cantilevered blade normal modes. The effect of the displacement at the boundary between the disk and the blades is also included in the formulation. To capture the motion at the disk-blade interface, other modes (in addition to the normal cantilevered blade modes) are required. However, these additional modes (constraint modes) can be neglected for small motions at the disk-blade interfaces.

In CMM, the motion of the  $n^{\text{th}}$  blade portion of the tuned-system modes is described by cantilevered blade normal modes and constraint modes as

$$\Phi_{\Gamma,n}^S = \begin{cases} \begin{bmatrix} \Phi_o^B & \Psi_o^{B,m} \\ \mathbf{0} & \mathbf{I} \end{bmatrix} \begin{bmatrix} \mathbf{q}_{\phi,n}^m \\ \mathbf{q}_{\psi,n}^m \end{bmatrix} & \text{for mass mistuning,} \\ \begin{bmatrix} \Phi_o^B & \Psi_o^{B,k} \\ \mathbf{0} & \mathbf{I} \end{bmatrix} \begin{bmatrix} \mathbf{q}_{\phi,n}^k \\ \mathbf{q}_{\psi,n}^k \end{bmatrix} & \text{for stiffness mistuning,} \end{cases} \quad (1)$$

where  $\Phi_{\Gamma,n}^S$  is the portion of the tuned system modes corresponding to the  $n^{\text{th}}$  blade,  $\Phi_o^B$  represents the tuned cantilevered blade normal modes,  $\Psi_o^{B,k}$  and  $\Psi_o^{B,m}$  represent the cantilevered blade constraint modes for the stiffness and mass matrices,  $\mathbf{q}_{\phi}^k$  and  $\mathbf{q}_{\phi}^m$  are the modal participation factors of the cantilevered blade normal modes related to the stiffness and mass matrices, and  $\mathbf{q}_{\psi}^k$  and

$\mathbf{q}_{\psi}^m$  are the modal participation factors of the constraint modes related to the stiffness and mass matrices.

When the displacements at the blade-disk interfaces are very small the contribution of the constraint modes to the mistuning projection can be neglected. This means that only the interior DOF of each blade have to be considered while computing the stiffness and mass mistuned matrices. Further, the mistuned mass and stiffness matrices of the  $n^{\text{th}}$  blade can be approximated as the mistuned mass and stiffness matrices of a cantilevered blade fixed at its root, i.e.  $\mathbf{M}_n^\delta \approx \mathbf{M}_{CB,n}^\delta$ , and  $\mathbf{K}_n^\delta \approx \mathbf{K}_{CB,n}^\delta$ . Matrices  $\mathbf{M}_n^\delta$  and  $\mathbf{K}_n^\delta$  are submatrices of the entire mass and stiffness mistuning matrices corresponding only to the interior DOF on the  $n^{\text{th}}$  blade. Matrices  $\mathbf{M}_{CB,n}^\delta$  and  $\mathbf{K}_{CB,n}^\delta$  are the mistuned stiffness and mass matrices of a cantilevered blade fixed at its root for the  $n^{\text{th}}$  blade. In all, there are  $N$  different mistuned cantilevered blade matrices, where  $N$  is the total number of blades of the blisk.

Since the constraint modes of a cantilevered blade can be neglected, the dominant cantilevered blade normal modes are enough to project mistuning without significant loss of accuracy in a given frequency range. Thus, the reduced stiffness and mass matrices for the mistuned blisk can be computed as

$$\begin{aligned} \boldsymbol{\mu}^{syn} &\approx \mathbf{I} + \sum_{n=1}^N \mathbf{q}_{\phi,n}^m T \boldsymbol{\mu}_{CB,n}^\delta \mathbf{q}_{\phi,n}^m, \\ \boldsymbol{\kappa}^{syn} &\approx \boldsymbol{\Lambda}^S + \sum_{n=1}^N \mathbf{q}_{\phi,n}^k T \boldsymbol{\kappa}_{CB,n}^\delta \mathbf{q}_{\phi,n}^k \end{aligned} \quad (2)$$

where,

$$\begin{aligned} \boldsymbol{\mu}_{CB,n}^\delta &= \Phi_o^{B,T} \mathbf{M}_{CB,n}^\delta \Phi_o^B, \\ \boldsymbol{\kappa}_{CB,n}^\delta &= \Phi_o^{B,T} \mathbf{K}_{CB,n}^\delta \Phi_o^B \end{aligned} \quad (3)$$

and  $\boldsymbol{\Lambda}^S$  is the diagonal matrix of the eigenvalues of the retained tuned system normal modes.

Matrices  $\boldsymbol{\mu}_{CB,n}^\delta$  and  $\boldsymbol{\kappa}_{CB,n}^\delta$  are full matrices in general. The coupling between the cantilevered blade modes due to mistuning is present in the off-diagonal terms of these matrices. Lim *et al.* [10] observed that usually one tuned cantilevered blade mode dominates the motion of each blade in the case of small mistuning, and hence each column of  $\mathbf{q}_{\phi,n}^m$  and  $\mathbf{q}_{\phi,n}^k$  is usually dominated by one modal participation factor. Thus, in a given frequency range the off-diagonal terms from the matrices  $\boldsymbol{\mu}_{CB,n}^\delta$  and  $\boldsymbol{\kappa}_{CB,n}^\delta$  can be neglected.

Finally, for small stiffness and mass mistuning, the equation of motion can be written as

$$[-\omega^2 \boldsymbol{\mu}^{syn} + (1 + j\gamma_{avg}) \boldsymbol{\kappa}^{syn}] \mathbf{p}_\phi^S = \Phi^{S,T} \mathbf{f}, \quad (4)$$

where  $\omega$  is the excitation frequency,  $\gamma_{avg}$  is the average structural damping coefficient for the entire blisk,  $\mathbf{f}$  is the physical forcing vector, and  $\mathbf{p}_\phi^S$  is the vector of modal coordinates. Note that the matrices used in Eqn. (4) are obtained from a FEM for a desired frequency range (which contains the tuned system modes).

### Modeling Blade to Blade Variability in Damping

In this section, the terms that model mistuning in damping are derived. The goal is to model variability in damping in the blades in a desired frequency range. Variations in the coefficient of structural damping within one blade are neglected. The variability in the damping in the blades can be expressed as a deviation from an average value of structural damping. This average value is arbitrary, and applies to the entire blisk. Let  $\mathbf{C}$  be the damping matrix of the entire blisk. One can write  $\mathbf{C}$  as a sum of two matrices:  $\mathbf{C}^S$  (which is the damping matrix of the tuned system) and  $\mathbf{C}^{S\delta}$  (which represents the mistuning in damping). Now, we define  $\gamma_{avg}$  as the average damping in the entire blisk, which is the same in all sectors. Note that  $\gamma_{avg}$  is also the structural damping coefficient of the tuned configuration, as seen in Eqn. (4). The structural damping matrix of the tuned blisk can be written as  $\mathbf{C}^S = j\gamma_{avg}\mathbf{K}^S$ , where  $\mathbf{K}^S$  is the stiffness matrix of the tuned system.

The projection of the damping matrix of the entire blisk onto the tuned system normal modes of the blisk can be expressed as

$$\begin{aligned}\Phi^{ST}\mathbf{C}\Phi^S &= \Phi^{ST}\mathbf{C}^S\Phi^S + \Phi^{ST}\mathbf{C}^{S\delta}\Phi^S, \\ \text{where} \\ \Phi^{ST}\mathbf{C}^S\Phi^S &= j\gamma_{avg}\Phi^{ST}\mathbf{K}^S\Phi^S = j\gamma_{avg}\Lambda^S\end{aligned}\quad (5)$$

with  $\Phi^S$  being the matrix of tuned system normal modes. Since damping mistuning is considered only in the blade portions of the blisk,  $\mathbf{C}^{S\delta}$  can be written as  $\mathbf{C}^{S\delta} = \sum_{n=1}^N \mathbf{C}_n^{\delta}$ , where  $\mathbf{C}_n^{\delta}$  is the damping mistuning matrix for the  $n^{\text{th}}$  blade. For the same reason the projection of  $\mathbf{C}^{S\delta}$  onto the normal modes of the blisk can be written using only the blade portions of the tuned system normal modes, which are given by  $\Phi_\Gamma^S$ . That yields

$$\Phi_\Gamma^{ST}\mathbf{C}^{S\delta}\Phi^S = \Phi_\Gamma^{ST}\mathbf{C}^\delta\Phi_\Gamma^S. \quad (6)$$

Thus, the projection of the damping mistuning matrix for the entire blisk using all the blade portions of the tuned system normal modes can be written as

$$\Phi_\Gamma^{ST}\mathbf{C}^\delta\Phi_\Gamma^S = \sum_{n=1}^N \Phi_{\Gamma,n}^{ST}\mathbf{C}_n^\delta\Phi_{\Gamma,n}^S. \quad (7)$$

Next, one defines  $\gamma_n$  as the structural damping coefficient for the  $n^{\text{th}}$  blade. We also define another variable  $\gamma_n^\delta$  as the deviation of

the damping coefficient of the  $n^{\text{th}}$  blade from  $\gamma_{avg}$ . Thus,  $\gamma_n^\delta$  is the quantity that models mistuning in damping in the  $n^{\text{th}}$  blade, and  $\gamma_n = \gamma_{avg} + \gamma_n^\delta$ . The structural damping matrix for the  $n^{\text{th}}$  blade can be written as

$$\mathbf{C}_n = j\gamma_n\mathbf{K}_n = j[\gamma_{avg} + \gamma_n^\delta]\mathbf{K}_n. \quad (8)$$

Here, the matrix  $\mathbf{K}_n$  is the stiffness matrix of the  $n^{\text{th}}$  blade, and it is the sum of the stiffness matrix of the  $n^{\text{th}}$  blade in the tuned configuration  $\mathbf{K}^S$  and the stiffness matrix  $\mathbf{K}_n^\delta$  which models the stiffness mistuning in the blades. The stiffness matrix of the  $n^{\text{th}}$  blade in the tuned configuration is a submatrix of  $\mathbf{K}^S$ , and the blade stiffness mistuning matrix  $\mathbf{K}_n^\delta$  is already incorporated into the ROM reviewed in the previous subsection. Note that the product  $\gamma_{avg}\mathbf{K}_n$  is a part of the reduced equation of motion in Eqn. (4), and hence it does not need to be included in the damping mistuning model again. From Eqn. (8), we use the terms that contain mistuning in damping only to obtain

$$\sum_{n=1}^N \mathbf{C}_n^\delta = \sum_{n=1}^N j\gamma_n^\delta\mathbf{K}_n. \quad (9)$$

Now we make the assumption that the damping mistuning matrix for small mistuning can be approximated by a mistuned cantilevered blade damping matrix as  $\mathbf{C}_n^\delta \approx \mathbf{C}_{CB,n}^\delta$ , where  $\mathbf{C}_{CB,n}^\delta$  represents the mistuned cantilevered blade damping matrix for the  $n^{\text{th}}$  blade. Thus, for an individual cantilevered blade,

$$\mathbf{C}_n^\delta \approx \mathbf{C}_{CB,n}^\delta = j[\gamma_n^\delta\mathbf{K}_{CB,n}^S + \gamma_n^\delta\mathbf{K}_{CB,n}^\delta]. \quad (10)$$

where  $\mathbf{K}_{CB,n}^S$  represents the tuned cantilevered blade stiffness matrix and  $\mathbf{K}_{CB,n}^\delta$  is the cantilevered blade mistuning stiffness matrix for the  $n^{\text{th}}$  blade.

Following Bladh *et al.* [15], the tuned cantilevered blade modes are used to project mistuning. Following a procedure similar to that in the previous sub-section where the contribution of the constraint modes of the cantilevered blade is neglected, one obtains

$$\Phi_{\Gamma,n}^S \approx \Phi_o^B \mathbf{q}_{\phi,n}^k. \quad (11)$$

where  $\mathbf{q}_{\phi,n}^k$  are the modal participation factors for the corresponding tuned cantilevered blade normal modes. Using Eqn. (10) and Eqn. (11) one can write Eqn. (7) as

$$\begin{aligned}\sum_{n=1}^N \Phi_{\Gamma,n}^{ST}\mathbf{C}_n^\delta\Phi_{\Gamma,n}^S &\approx \sum_{n=1}^N \Phi_{\Gamma,n}^{ST}\mathbf{C}_{CB,n}^\delta\Phi_{\Gamma,n}^S \\ &\approx j\sum_{n=1}^N \mathbf{q}_{\phi,n}^k{}^T \gamma_n^\delta \left\{ \Phi_o^{BT}\mathbf{K}_{CB,n}^S\Phi_o^B + \Phi_o^{BT}\mathbf{K}_{CB,n}^\delta\Phi_o^B \right\} \mathbf{q}_{\phi,n}^k.\end{aligned}\quad (12)$$

From Eqn. (12), one can identify that

$$\Phi_o^{BT} \mathbf{K}_{CB,n}^S \Phi_o^B = \Lambda_{CB,n}^S, \quad (13a)$$

where  $\Lambda_{CB,n}^S$  is the matrix of eigenvalues of a tuned cantilevered blade. Also, using Eqn. (3), one obtains

$$\Phi_o^{BT} \mathbf{K}_{CB,n}^\delta \Phi_o^B = \mathbf{k}_{CB,n}^\delta \approx \Lambda_{CB,n}^\delta, \quad (13b)$$

where the matrix defining mistuning in the cantilevered blade eigenvalues in Eqn. (3) (i.e.  $\mathbf{k}_{CB,n}^\delta$ ) is approximately equal to a diagonal matrix  $\Lambda_{CB,n}^\delta$  because the mistuned cantilevered blade matrix can be approximated as a diagonal matrix. Hence, one can write  $\Lambda_{CB,n}^\delta$  as the product of two diagonal matrices. One of them is the matrix of tuned cantilevered blade eigenvalues  $\Lambda_{CB,n}^S$ , and the other is defined as the diagonal matrix  $\delta_n$  of mistuning fractions for the eigenvalues of the  $n^{\text{th}}$  blade.

$$\Lambda_{CB,n}^\delta = \Lambda_{CB,n}^S \delta_n, \quad (14)$$

where the  $k^{\text{th}}$  diagonal value of the matrix  $\delta_n$  is the mistuning fraction for the  $k^{\text{th}}$  tuned cantilevered blade eigenvalue.

Eqns. (13a), (13b) and (14) are then combined with Eqn. (12) to obtain

$$\begin{aligned} & \sum_{n=1}^N \Phi_{\Gamma,n}^S{}^T \mathbf{C}_n^\delta \Phi_{\Gamma,n}^S \\ & \approx j \sum_{n=1}^N \mathbf{q}_{\phi,n}^k{}^T \left\{ \gamma_n^\delta \Lambda_{CB,n}^S + \gamma_n^\delta \Lambda_{CB,n}^S \delta_n \right\} \mathbf{q}_{\phi,n}^k. \end{aligned} \quad (15)$$

To consider effects of damping mistuning on the response of the entire blisk, one adds Eqn. (15) to Eqn. (4) to obtain

$$\left[ -\omega^2 \boldsymbol{\mu}^{\text{syn}} + (1 + j\gamma_{\text{avg}}) \mathbf{k}^{\text{syn}} \right] \mathbf{p}_\phi^S + \sum_{n=1}^N \Phi_{\Gamma,n}^S{}^T \mathbf{C}_n^\delta \Phi_{\Gamma,n}^S = \Phi^S{}^T \mathbf{f},$$

or

$$\begin{aligned} & \left[ -\omega^2 \boldsymbol{\mu}^{\text{syn}} + (1 + j\gamma_{\text{avg}}) \mathbf{k}^{\text{syn}} \right] \mathbf{p}_\phi^S + \\ & j \left\{ \sum_{n=1}^N \mathbf{q}_{\phi,n}^k{}^T \left[ \gamma_n^\delta \Lambda_{CB,n}^S + \gamma_n^\delta \Lambda_{CB,n}^S \delta_n \right] \mathbf{q}_{\phi,n}^k \right\} \mathbf{p}_\phi^S = \Phi^S{}^T \mathbf{f}. \end{aligned} \quad (16)$$

Now, one can substitute the matrix  $\mathbf{k}^{\text{syn}}$  from Eqn. (16) using Eqn. (2). Note that here,  $\mathbf{k}_{CB,n}^\delta$  was again approximated by  $\Lambda_{CB,n}^\delta$ . Finally, using Eqn. (14) one can write Eqn. (16) as

$$\begin{aligned} & \left[ -\omega^2 \boldsymbol{\mu}^{\text{syn}} + (1 + j\gamma_{\text{avg}}) \Lambda^S \right] \mathbf{p}_\phi^S + j \left\{ \sum_{n=1}^N \mathbf{q}_{\phi,n}^k{}^T \gamma_n^\delta \Lambda_{CB,n}^S \mathbf{q}_{\phi,n}^k \right\} \mathbf{p}_\phi^S \\ & + \left\{ \sum_{n=1}^N \mathbf{q}_{\phi,n}^k{}^T (1 + j\gamma_{\text{avg}}) \Lambda_{CB,n}^S \delta_n \mathbf{q}_{\phi,n}^k \right\} \mathbf{p}_\phi^S \\ & + j \left\{ \sum_{n=1}^N \mathbf{q}_{\phi,n}^k{}^T \gamma_n^\delta \Lambda_{CB,n}^S \delta_n \mathbf{q}_{\phi,n}^k \right\} \mathbf{p}_\phi^S = \Phi^S{}^T \mathbf{f}. \end{aligned} \quad (17)$$

Equation (17) represents a new ROM that captures variability in damping from blade to blade along with stiffness mistuning. Factoring out the diagonal matrix  $\Lambda_{CB,n}^S$ , one may group the terms which are a part of all the summations used in Eqn. (17)

$$\mathbf{q}_{\phi,n}^k{}^T \Lambda_{CB,n}^S \left[ (1 + j\gamma_{\text{avg}}) \delta_n + j\gamma_n^\delta + j\gamma_n^\delta \delta_n \right] \mathbf{q}_{\phi,n}^k, \quad (18)$$

where,  $\gamma_n^\delta$  is a diagonal matrix with diagonal values equal to  $\gamma_n^\delta$ .

Now, consider the terms inside the square brackets in Eqn. (18) above. A combined mistuning matrix can be written for these terms (for the  $n^{\text{th}}$  blade) as

$$\mathbf{m}_n^{\text{comb}} = (1 + j\gamma_{\text{avg}}) \left[ \delta_n + \frac{j\gamma_n^\delta (\mathbf{I} + \delta_n)}{(1 + j\gamma_{\text{avg}})} \right]. \quad (19)$$

The matrix  $\mathbf{m}_n^{\text{comb}}$  can be viewed as a general mistuning matrix consisting of complex quantities (as opposed to the matrix  $\delta_n$  which has only real values).

Equation (17) can then be rewritten using Eqn. (19) to provide a concise representation of the ROM as

$$\begin{aligned} & \left[ -\omega^2 \boldsymbol{\mu}^{\text{syn}} + (1 + j\gamma_{\text{avg}}) \Lambda^S \right] \mathbf{p}_\phi^S \\ & + \left[ \sum_{n=1}^N \mathbf{q}_{\phi,n}^k{}^T \Lambda_{CB,n}^S \mathbf{m}_n^{\text{comb}} \mathbf{q}_{\phi,n}^k \right] \mathbf{p}_\phi^S = \Phi^S{}^T \mathbf{f}. \end{aligned} \quad (20)$$

To perform simulations using the new ROM for damping mistuning (but with no mass and stiffness mistuning) a simplified form of the ROM can be used. Specifically, the fraction inside the square brackets of Eqn. (19) can be expanded as follows,

$$\frac{j\gamma_n^\delta [\mathbf{I} + \delta_n]}{(1 + j\gamma_{\text{avg}})} = \gamma_{\text{avg}} \gamma_n^\delta \frac{[\mathbf{I} + \delta_n]}{1 + \gamma_{\text{avg}}^2} + j\gamma_n^\delta \frac{[\mathbf{I} + \delta_n]}{1 + \gamma_{\text{avg}}^2}. \quad (21)$$

Since stiffness mistuning is absent, the matrix  $\delta_n$  is zero and Eqn. (21) reduces to

$$\frac{j\gamma_n^\delta [\mathbf{I} + \delta_n]}{(1 + j\gamma_{\text{avg}})} = \frac{\gamma_{\text{avg}} \gamma_n^\delta}{1 + \gamma_{\text{avg}}^2} + j \frac{\gamma_n^\delta}{1 + \gamma_{\text{avg}}^2}. \quad (22)$$

The values of the damping coefficients  $\gamma_n$  in every blade of the blisk (and hence the matrix of the deviations of the damping coefficients  $\gamma_n^\delta$ ) are taken to be of the order of  $10^{-4}$ . Hence, in Eqn. (22), the real part of the right hand side is much smaller than the imaginary part and hence can be neglected. The real part is physically a stiffness-like mistuning induced by damping mistuning. However, this does not mean that there is any correlation between stiffness mistuning and damping mistuning. The two variables are independent. Also, the fact that the real part of Eqn. (22) is not zero indicates that structural damping variability can lead to mistuning which appears to be stiffness-like

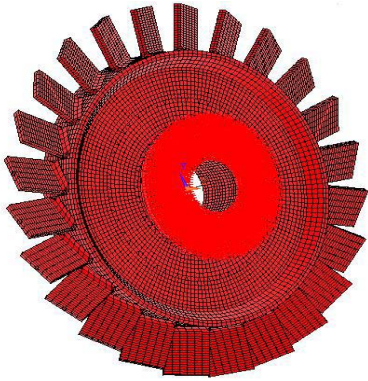


FIGURE 1. FINITE ELEMENT MODEL OF THE BLISK.

(and leads to variations in system-level resonant frequencies). Nonetheless, that effect is small (second order), and hence it is negligible especially for lightly damped structures. The denominator of the imaginary part of right hand side of Eqn. (22) has a term  $\gamma_{avg}^2$  which can also be neglected because  $\gamma_{avg}^2 \ll 1$ . Thus a very simple form of Eqn. (22) is obtained and can be combined with Eqn. (19) and Eqn. (20) to obtain a ROM for damping mistuning as

$$\begin{aligned} & [-\omega^2 \mathbf{I} + (1 + j\gamma_{avg}) \mathbf{\Lambda}^S] \mathbf{p}_\phi^S \\ & + j(1 + j\gamma_{avg}) \left[ \sum_{n=1}^N \mathbf{q}_{\phi,n}^k \mathbf{\Lambda}_{CB,n}^S \gamma_n^S \mathbf{q}_{\phi,n}^k \right] \mathbf{p}_\phi^S = \mathbf{\Phi}^S T f. \end{aligned} \quad (23)$$

## RESULTS

This section presents two sets of results. First, the results validating the proposed ROM are presented. Next, forced responses obtained using the novel ROM for various damping mistuning patterns are presented. A statistical analysis for various damping mistuning patterns having different standard deviations is presented.

### ROM Validation

The results obtained by simulations of a full FEM in ANSYS were compared with the results obtained using the novel ROMs. A very good agreement was found.

The FEM was developed in ANSYS, with all SOLID45 elements having structural damping. Figure 1 shows the full size FEM in ANSYS. The blisk model has 24 blades and 141,120 DOF. The equation used by ANSYS to model structural damping at a component level is  $\mathbf{C}_c = \left( \frac{\beta_c}{\omega} \right) \mathbf{K}_c$ , where  $\mathbf{K}_c$  is the stiffness matrix of component  $c$ ,  $\beta_c$  is the structural damping coefficient of the component,  $\omega$  is the frequency of excitation, and  $\mathbf{C}_c$  is the damping matrix of component  $c$ .

To calculate the forced response of the blisk, travelling wave excitations were used to force the blades. For a travelling wave

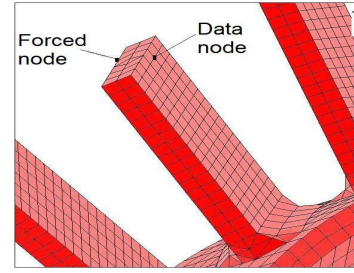
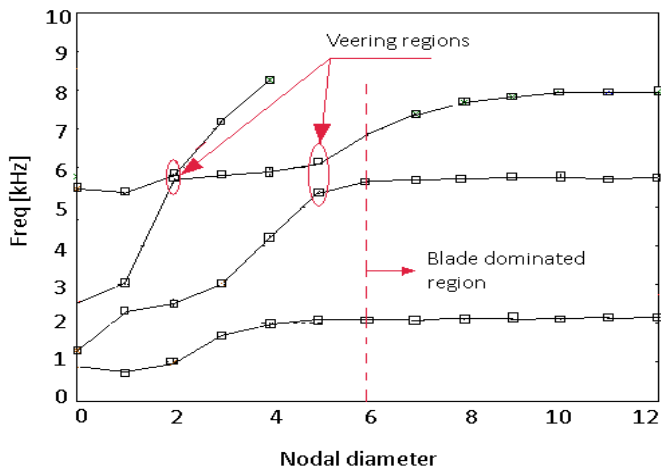


FIGURE 2. ONE OF THE BLADES; THE NODE BEING FORCED AND THE NODE AT WHICH DISPLACEMENT IS CALCULATED.

excitation, the force on the  $n^{\text{th}}$  blade of a blisk with  $N$  blades can be written as  $\mathbf{F}_n = |F| e^{i\sigma_n}$ , where  $\sigma_n = \frac{2\pi E(n-1)}{N}$  is the phase of the load applied to the  $n^{\text{th}}$  blade,  $E$  is the engine order excitation and  $|F|$  is the magnitude of the physical force applied to the blades. The blades were loaded parallel to the axis of the blisk. The displacement of the blades in the direction of the applied forces was monitored (because it is dominant when compared to displacements in other directions). Figure 2 shows one of the blades. Two nodes are marked in the figure. The force was applied at one of the marked nodes, and the displacement was calculated at the other node. Two such nodes were selected on every blade in a cyclically symmetric manner.

The veering regions are the regions where blade dominated modes of the blisk are close to the disk dominated modes. A high degree of coupling between blade dominated and disk dominated modes is present in the veering regions. Thus, a mixed disk-blade motion is exhibited in the veering region. Also, due to disk motion there is a lot of energy exchange between blades which may lead to the vibration energy being localized in a certain blade or group of blades [46]. Veering regions pose a good challenge to the accuracy of a ROM. Hence, for validation, the frequency range of 5 – 7 kHz and the engine order excitations 2 and 5 were selected, so that modes in the veering regions (shown in Fig. 3) were excited.

There are various mechanisms by which energy is dissipated in blisks. Thus, the damping coefficients used in models are often inaccurate. That is particularly important when damping coatings are used. In those cases, small errors in the coating thickness can also lead to large relative variations in damping amongst the blades. Hence, the interest here lies in understanding the effects of large variations in damping values between the approximate values used in models and real values. Specifically, the variation in the damping values amongst the blades was taken to be  $\pm 80\%$  of the average value  $\gamma_{avg}$ . The value of the structural damping coefficient for each blade was selected from a uniform distribution over the interval bounded by the maximum variation over the average damping of the entire blisk. Also, the variation in the damping coefficients was chosen such that it had a zero mean



**FIGURE 3.** NATURAL FREQUENCIES VS. NODAL DIAMETER FOR THE TUNED BLISK (ANSYS RESULTS).

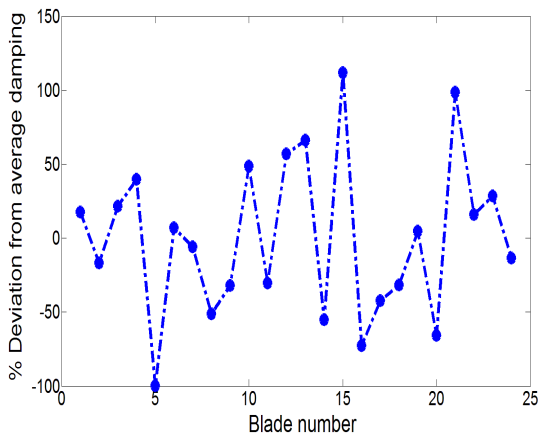


**FIGURE 4.** DAMPING MISTUNING PATTERN.

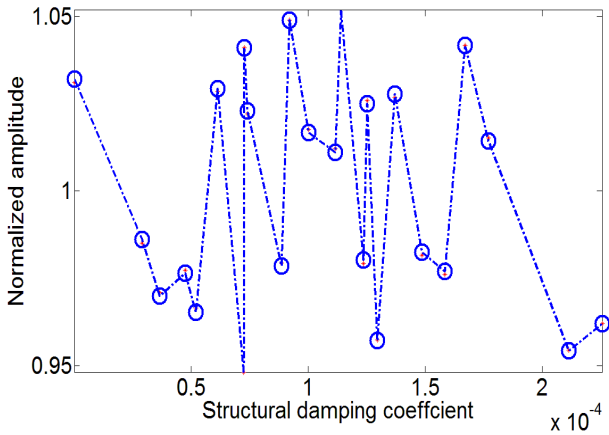
value. This means that the average value of the damping coefficients in all the blades is equal to the damping value of a tuned blisk. Figure 4 shows one of the damping mistuning patterns used.

The ROMs were first tested to confirm convergence in the frequency range of interest. Specifically, convergence of the ROM is guaranteed if a large enough number of tuned system normal modes and cantilevered blade modes are used. These numbers of modes (define the size of the ROM and) are easily chosen by using the range of frequencies of interest. If for example, one constructs a ROM with all modes in a range 0-14 kHz and then uses it for predictions in a range 0-7 kHz, then it is clear that convergence is ensured. Including a larger num-

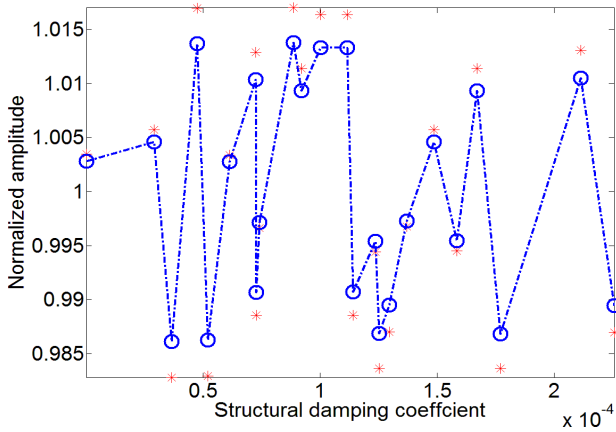
ber of modes than required would only increase the size of the ROM and provide essentially the same answers in the 0-7 kHz range. Also, since converged models were used, their sensitivity to including more modes is also negligible. The results obtained from the FEM and the novel ROM are compared in Fig. 5. The amplitude of the node on each blade was normalized by the average amplitude of all blades at that particular resonant response in Fig. 5. Figure 5 shows that the results from ANSYS and the ROM match very closely. The maximum error for engine order excitation 2 is 0.11%, while for engine order excitation 5 it is 0.3%. The novel ROM works accurately and captures these variations very accurately and at all engine orders. The normalized amplitude for the  $n^{\text{th}}$  blade node is plotted in Fig. 5 against the corresponding structural damping coefficient  $\gamma_n$  to determine if any correlation exists between the damping value  $\gamma_n$  and the normalized amplitude of the  $n^{\text{th}}$  blade node. The observed variation in the normalized amplitudes is 5% for engine order excitation 2, and 2% for engine order excitation 5. Also, there is no strong correlation between the damping value  $\gamma_n$  and the normalized amplitude of the  $n^{\text{th}}$  blade.

Next, one may investigate the effects of damping mistuning on the variation of the blade amplitudes at all engine order excitations using the validated ROMs. Specifically, the results shown in Fig. 6 reveal that there is no strong correlation between the variation in the normalized amplitudes and the engine order excitation. Furthermore, even though intuitively one may consider that the response of a component is inversely proportional only to its own damping capacity, this is not true as seen from the results. Some of the blades with higher damping coefficients have a larger response than the blades having much smaller damping coefficients. That is because a variation in the physical property of a component affects the entire system and not just the individual component. This observation is not novel. It matches similar observations made precisely by Petrov [3], Petrov *et al.* [2, 4] and Elliot *et al.* [5].

The ROM is accurate in the presence of combined stiffness and damping mistuning as well. Figure 7 shows that the errors in the predicted amplitude and the resonant frequencies of all blades for engine order excitations 2 and 5 are small. Since both stiffness and damping mistuning are present, Eqn. (20) is used to obtain the results in Fig. 7. The stiffness mistuning pattern is shown in Fig. 8. The damping mistuning pattern is the same as the one used to obtain the results in Fig. 5.



(a) ENGINE ORDER EXCITATION 2



(b) ENGINE ORDER EXCITATION 5

**FIGURE 5.** NORMALIZED AMPLITUDE OF ONE NODE PER BLADE VS. CORRESPONDING STRUCTURAL DAMPING COEFFICIENT FOR EACH BLADE USING THE NOVEL ROM ('\*') AND USING ANSYS ('O-') WITH DAMPING MISTUNING.

### Statistical Analysis using ROMs

Next, the validated ROMs are used to calculate the forced response of the blisk using a large number of damping mistuning patterns with different standard deviations. For every mistuning pattern, the mean value of the damping coefficients in all the blades is equal to that of a tuned blisk. This helps to define a blade amplification factor for every response obtained using the different mistuning patterns. Here, the blade amplification factor is defined as the ratio of the maximum amplitude of the cyclic nodes on all the blades in the mistuned blisk to the amplitude of the same set of cyclic nodes from a tuned blisk.

Figure 9 shows results for engine order excitation 2. An average value of  $1 \times 10^{-4}$  was used for 1,000 different values of

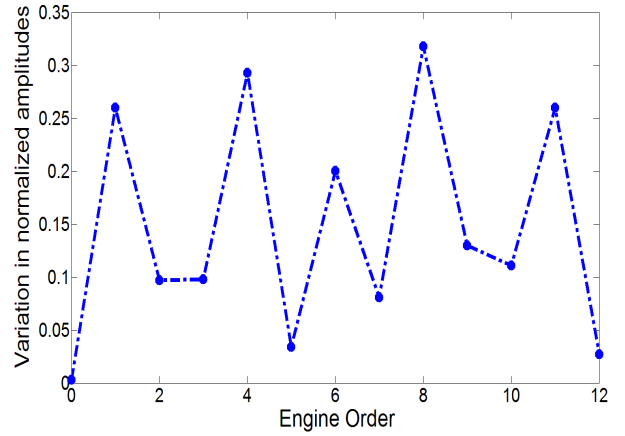
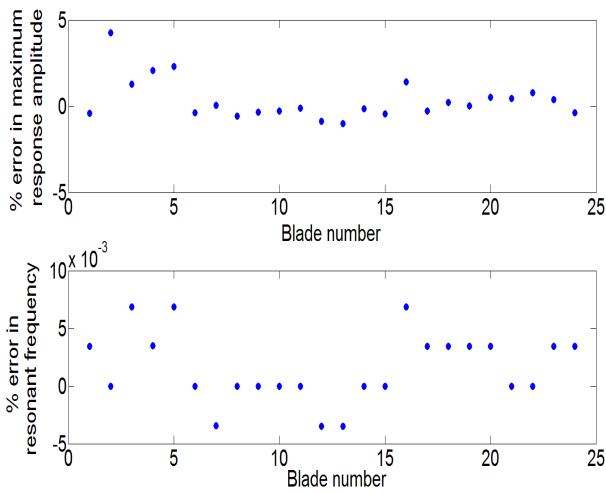


**FIGURE 6.** VARIATION IN THE NORMALIZED AMPLITUDE OF ALL BLADES VS. ENGINE ORDER EXCITATION.

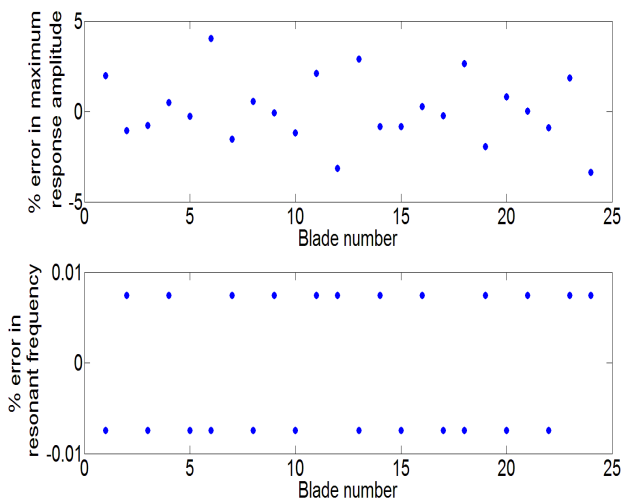
the standard deviation of the damping mistuning pattern ranging from 0 to  $2 \times 10^{-4}$  (0% to 100% of the average damping value). For each value of standard deviation, 5,000 random damping mistuning patterns are input to the novel ROM. For each pattern of mistuning, a blade amplification factor is calculated, and plotted as a dense cloud of points in Fig. 9. Thus, a random distribution of 5,000 different blade amplification factors is computed for each standard deviation of the damping mistuning. These Monte-Carlo simulations were performed for a lower number of samples (e.g. 2,000) and it was observed that the results are essentially the same. Hence, the larger number of samples (5,000 samples) was used for each of the calculations to ensure that the statistical results are robust. The ability to use such a very large number of samples (due to an extreme computational efficiency) highlights one of the benefits the proposed reduced order modeling method provides.

The results in Fig. 9 show that the mean value and the corresponding standard deviation of the blade amplification factors increase with an increase in the standard deviation of the damping mistuning. Hence, the distribution of the amplification factors widens with an increase in the standard deviation of mistuning. The line of the 99<sup>th</sup> percentile is also shown in Fig. 9.

The probability density function for the distribution of blade amplification factors for all standard deviations of mistuning can be computed also. For example, Fig. 10 shows the three dimensional plot of the probability density function of the blade amplification factor against the standard deviation of the damping mistuning for engine order excitation 2. One may note in Fig. 10 that, interestingly, the maximum probability of obtaining a particular blade amplification factor does not bear a correlation with the standard deviation of the damping mistuning. Also, the value of the blade amplification factor which has the maximum



(a) ENGINE ORDER EXCITATION 2



(b) ENGINE ORDER EXCITATION 5

**FIGURE 7.** COMPARISON OF RESULTS OBTAINED USING THE NOVEL ROM AND THE RESULTS OBTAINED USING ANSYS WHEN BOTH STIFFNESS AND DAMPING MISTUNING ARE PRESENT.

probability of occurrence increases with an increase in the standard deviation of the damping mistuning. Furthermore, similar to Fig. 9, Fig. 10 highlights that the distribution of the blade amplification factors widens as with an increase in the standard deviation of the damping mistuning increases. Note that in Fig. 10, the probability for a standard deviation of zero, corresponding to a tuned blisk has not been plotted (to compare the distributions only for the mistuned case).

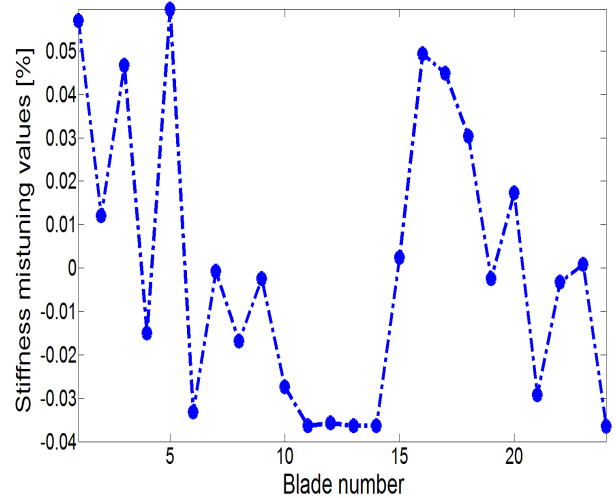


**FIGURE 8.** STIFFNESS MISTUNING PATTERN SHOWING THE STIFFNESS MISTUNING FRACTIONS FOR EACH BLADE.

Next, the ROMs were used to perform similar statistical analyses at all engine order excitations. The characteristics pertaining to the mean value, the standard deviation and the 99<sup>th</sup> percentile of the blade amplification factors for all the engine order excitations were found to be similar to those obtained for engine order excitation 2. The median values for all the engine orders are shown in Fig. 11. These results show that, for all of the engine order excitations, the median blade amplification factor increases with an increase in the standard deviation of the damping mistuning. Also, there is no strong correlation between the engine order excitation and the corresponding median blade amplification factors. Furthermore, at every engine order excitation, the results for the median values show characteristics similar to those observed in Fig. 9 for engine order excitation 2. Note that a total of 5,000,000 computations were performed to obtain the results in Fig. 10 and 65,000,000 computations to obtain the results in Fig. 11. Such a large number of computations were possible because of the use of the novel ROMs.

A statistical analysis was performed on a different blisk with different number of blades (23) and different disk to blade coupling. The results obtained for all the engine order excitations are presented in Fig. 12. As expected, the results show different values of blade amplification factors but the way in which the blade amplification factors are scattered for all the standard deviations of the damping mistuning pattern are similar to those obtained using the 24 bladed blisk. Further, similar to the blisk with 24 blades there is no strong correlation between the engine order excitation and the blade amplification factors, as seen from Fig. 12.

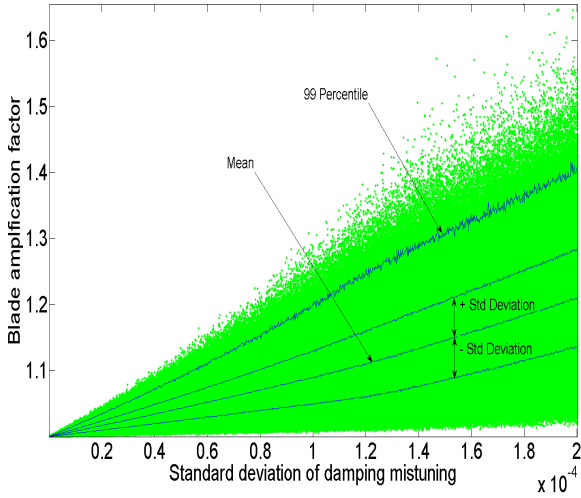


**FIGURE 9.** RESULTS OBTAINED USING THE NOVEL ROM FOR STATISTICAL ANALYSIS. RESULTS FOR ENGINE ORDER 2 ARE SHOWN. THE LINES OF MEAN VALUE, STANDARD DEVIATION FROM THE MEAN AND THE 99<sup>TH</sup> PERCENTILE OF THE BLADE AMPLIFICATION FACTOR AT ALL VALUES OF STANDARD DEVIATION ARE SHOWN.

## DISCUSSION AND CONCLUSIONS

Novel ROMs were developed to model damping mistuning. The damping in the blades was modeled as structural damping. The use of structural damping in general has been validated in a variety of publications [27, 29, 30, 39] and in particular by the analysis and validation of the CMM approach [10, 40] This paper presents an extension to those studies, where damping was considered structural at a system level (and hence damping mistuning was ignored). The damping coefficients were considered distinct for each blade. This means that the damping is structural only at the blade level. When all the individual blade damping matrices are assembled together, the global structural damping matrix cannot be defined using one value of  $\gamma$ . Thus, the damping in the blisk as a whole cannot be defined as structural damping. A single structural damping coefficient (scalar value) was used to characterize damping in each blade in a frequency range of interest. Variation in damping within a single blade was not considered. If a real system exhibits damping which does not closely follow the assumptions of structural damping, then one alternate approach (used in the past) is to define different damping coefficients in different frequency ranges. The method proposed can be used in a similar fashion. Note that in various frequency ranges, the structural damping coefficients do not have to be the same values for each blade. Hence, the damping mistuning does not have to be the same in all frequency ranges. Thus, the methodology presented here is not limited to characterizing damping with

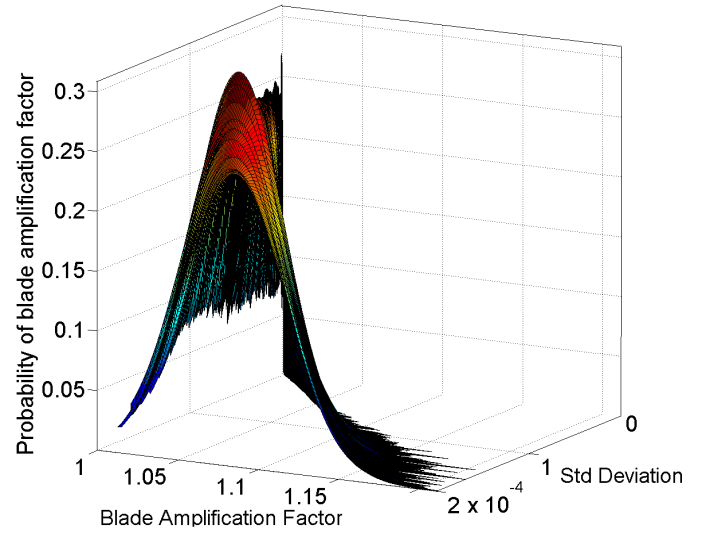


**FIGURE 10.** PROBABILITY DENSITY FUNCTION PLOTTED USING THE RESULTS OBTAINED FROM USING THE NOVEL ROM; FOR DEMONSTRATION PURPOSES THE PLOT FOR ENGINE ORDER 2 IS SHOWN.

a single scalar for all frequencies.

One of the ways of characterizing damping effects is by evaluating an equivalent modal damping value for each mode. That can be useful when the damping matrix is diagonal in the modal coordinates. A diagonal structure shows that there is no energy exchange amongst the various modes. However, the damping matrix obtained in this novel ROM has non-zero off-diagonal elements and is not even diagonally dominant. This shows that there exists energy exchange between different modes due to damping mistuning. Hence, it will not be accurate to model accurately the damping mistuning as variations in modal damping values.

A FEM of a blisk was used to validate the novel ROMs. A maximum error of 0.3% between the amplitudes predicted by a ROM and the FEM was found for the case where only damping mistuning is present. When stiffness mistuning was included along with damping mistuning, a maximum error of 0.007% was obtained for the estimates of the resonant frequencies, and a maximum error of 4% for the amplitude of the resonant response. These errors are consistent with the errors obtained using CMM (i.e. with no damping mistuning). They are caused by the various approximations in CMM, such as the fact that  $\mathbf{\kappa}_{CB,n}^\delta \approx \mathbf{\Lambda}_{CB,n}^\delta$  and that the constrained modes  $\Psi_o^{B,m}$  and  $\Psi_o^{B,k}$  have negligible effects.

The novel ROMs are very simple to use and mathematically similar to the CMM model developed by Lim *et al.* [10]. The similarity comes from the fact that the equations for the ROM are alike. Thus, the novel ROMs can be very easily generalized and used to model not only damping mistuning, but also stiffness

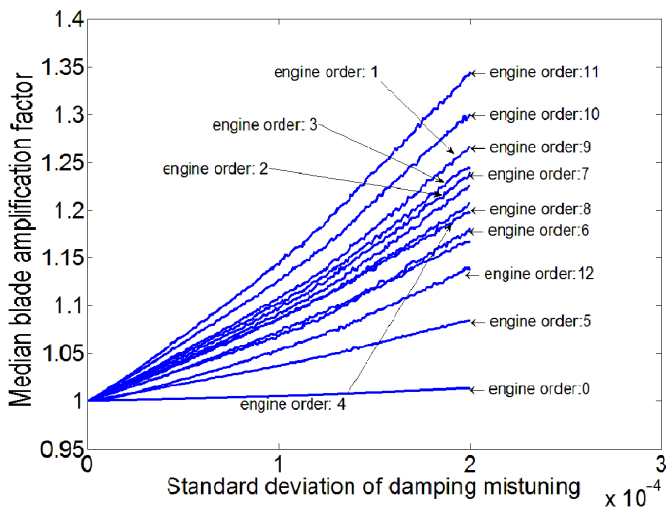


**FIGURE 11.** BLISK WITH 24 BLADES: LINES OF MEDIAN BLADE AMPLIFICATION FACTORS VS. STANDARD DEVIATION OF MISTUNING PATTERN FOR ALL ENGINE ORDER EXCITATIONS.

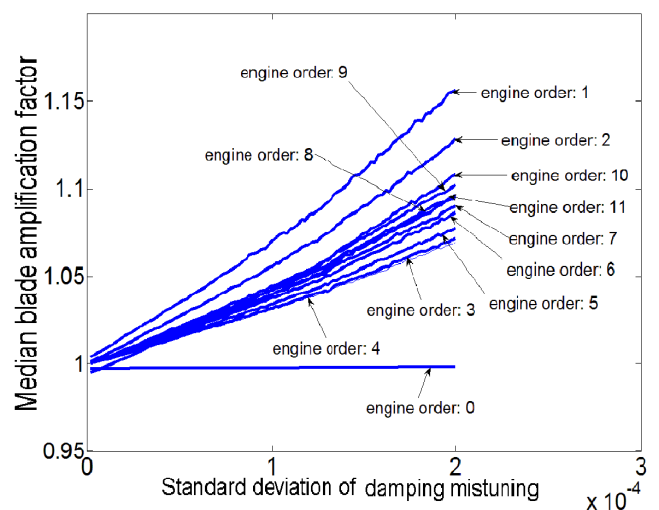


**FIGURE 12.** BLISK WITH 23 BLADES: LINES OF MEDIAN BLADE AMPLIFICATION FACTORS VS. STANDARD DEVIATION OF MISTUNING PATTERN FOR ALL ENGINE ORDER EXCITATIONS.

mistuning. The CMM methodology has been used successfully for both proportional and non-proportional mistuning [10,40]. In particular, CMM has been used to model non-proportional stiffness mistuning, but in those cases the resulting ROMs have larger sizes. The same range of validity observed for CMM holds for the proposed approach as well. The proposed method adds to CMM the ability to model damping mistuning.

In general, for systems with structural damping, the natural frequencies are resonant frequencies. In contrast, the analysis provided in this paper highlights a somewhat counter-intuitive result. It is seen that mistuning is a real quantity in the case of only stiffness mistuning and a complex quantity in the case of damping mistuning. Due to damping mistuning alone, there exists an induced stiffness-like mistuning which is seen in the real part of Eqn. (22). However, this does not mean that stiffness mistuning and damping mistuning are correlated. The fact that the real part of Eqn. (22) is not zero provides the intriguing result that structural damping variability can lead to mistuning which appears to be stiffness-like (and leads to variations in system-level resonant frequencies) even if the stiffness mistuning is zero. Nonetheless, that effect is small (second order), and hence it is negligible especially for lightly damped structures.

Elliot *et al.* [5] have observed that the damping capacity of an individual component affects the response of the adjacent blades as well. In that paper friction dampers have been used, and dampers at certain locations have been removed to simulate excessive wear. A similar phenomenon is revealed by the results obtained using the new methodology. However, the overall

bladed disk model, the damping model, and the source of damping mistuning are very different between this work and that of Elliot *et al.* [5]. In particular, one may note that the methodology used here to model damping variability is novel and clearly distinct from previous studies. This novel methodology is based on CMM, and it is a reduced order modeling approach which provides significant computational savings (reducing computational costs by orders of magnitude). The fact that this novel (computationally efficient) methodology makes predictions similar to other existing predictions is reassuring. In addition, the methodology makes new predictions also, e.g. the fact that there is no strong correlation between the engine order of the excitation and the amount of variation in the blade amplitudes.

The computational efficiency of the new methodology presented in this paper enables the fast simulation of huge numbers of damping mistuning cases. The novel ROM was thus used to perform a statistical analysis to characterize the effects of random damping mistuning patterns. The blade amplification factors were calculated for many mistuning patterns with different standard deviations. The results show that for all random damping mistuning patterns with the same standard deviation, a random distribution of blade amplification factors can be obtained. As the standard deviation of the mistuning increases, the median, mean and the standard deviation of the distribution of the blade amplification factors also increases. This is true in general for all the engine order excitations. There is, however, no strong correlation between the engine order and the distribution of the blade amplification factors. Note that, such a statistical analysis can

be helpful to determine the probability of the occurrence of certain blade amplification factors if the standard deviation of the mistuning pattern is known.

Petrov *et al.* [2, 4] and Petrov [3] reported on the scatter in the blade amplitudes due to scatter (of up to 20%) in the various characteristics of underplatform dampers. However, an analysis using different values of maximum variation and different standard deviations of the damping mistuning pattern was not performed. The computational efficiency of the CMM-based method herein enabled an extensive calculation and analysis using a large number of damping mistuning patterns each with different maximum variations (as high as 80%) for various values of the standard deviation. In addition, a statistical analysis at all the engine order excitations was included herein to complement results presented in previous work.

## ACKNOWLEDGMENT

The partial financial support of the Air Force Office of Scientific Research through grant FA9550-08-1-0276 (Dr. Douglas Smith, Program Manager) is gratefully acknowledged.

## REFERENCES

- [1] Yan, Y. J., Cui, P. L., and Hao, H. N., 2008. "Vibration mechanism of a mistuned bladed-disk". *Journal of Sound and Vibration*, **317**(1-2), October, pp. 294–307.
- [2] Petrov, E. P., and Ewins, D. J., 2005. "Method for analysis of nonlinear multiharmonic vibrations of mistuned bladed disks with scatter of contact interface characteristics". *Journal of Turbomachinery*, **127**, January, pp. 128–136.
- [3] Petrov, E. P., 2007. "A sensitivity-based method for direct stochastic analysis of nonlinear forced response for bladed discs with friction interfaces". *Proceedings of GT2007 ASME Turbo Expo 2007: Power for Land, Sea and Air*, May.
- [4] Petrov, E. P., and Ewins, D. J., 2005. "Effects of mistuning on the forced response of bladed discs with friction dampers". *Evaluation, Control and Prevention of High Cycle Fatigue in Gas Turbine Engines for Land, Sea and Air Vehicles Meeting Proceedings RTO-MP-AVT-121*(38), October, pp. 1–16.
- [5] Elliot, B., Wardle, M. E., and Bellamy, D. R. A., 2008. "A study of the effect of non-linear damping on mistune behavior of a turbine rotor". *Proceedings of ASME Turbo Expo 2008: Power for Land, Sea and Air*, June.
- [6] Muszynska, A., and Jones, D. I. G., 1983. "On tuned bladed disk dynamics: some aspects of friction related mistuning". *Journal of Sound and Vibration*, **86**(1), pp. 107–128.
- [7] He, Z., Epureanu, B. I., and Pierre, C., 2008. "Convergence predictions for aeroelastic calculations of tuned and mistuned bladed disks". *Journal of Fluids and Structures*, **24**(5), July, pp. 732–749.
- [8] He, Z., Epureanu, B. I., and Pierre, C., 2007. "Parametric study of the aeroelastic response of mistuned bladed disks". *Computers and Structures*, **85**(11-14), June-July, pp. 852–865.
- [9] He, Z., Epureanu, B. I., and Pierre, C., 2007. "Fluid-structural coupling effects on the dynamics of mistuned bladed disks". *AIAA Journal*, **45**(3), March, pp. 552–561.
- [10] Lim, S.-H., 2005. "Dynamic analysis and design strategies for mistuned bladed disks". Phd thesis, University of Michigan, Ann Arbor, MI.
- [11] Xiao, B., Rivas-Guerra, A. J., and Mignolet, M. P., 2004. "Maximum amplification of blade response due to mistuning in multi degree of freedom blade models". *Proceedings of ASME Turbo Expo 2004 Power for Land, Sea, and Air*, **6**, June 14-17, pp. 427–438.
- [12] Martel, C., and Corral, R., 2009. "Asymptotic description of maximum mistuning amplification of bladed disk forced response". *Journal of Engineering for Gas Turbines and Power*, **131**(2), March, pp. 022506.1–022506.10.
- [13] Shin, S. H., Kang, M. K., and Yoo, H. H., 2008. "Mistuned coupling stiffness effect on the vibration localization of cyclic systems". *Journal of Mechanical Science and Technology*, **22**(2), pp. 269–275.
- [14] Lee, K.-C., Li, K.-C., Yu, H. H., and Lin, C.-C., 2006. "Forced response of harmonic mistuned blade disks". *Key Engineering Materials*, **324-325**(145), November, pp. 145–148.
- [15] Bladh, R., Castanier, M. P., and Pierre, C., 1999. "Reduced order modeling and vibration analysis of mistuned bladed disk assemblies with shrouds". *ASME Journal of Engineering for Gas Turbines and Power*, **121**(3), July, pp. 515–522.
- [16] Kruse, M., and Pierre, C., 1996. "Forced response of mistuned bladed disks using reduced-order modeling". *Proceedings of the 37th AIAA/ASME/ASCE/AHS/ASC Structures, Structural Dynamics and Materials Conference and Exhibit*, April 15-17, pp. 1938–1950.
- [17] Wei, S.-T., and Pierre, C., 1990. "Statistical analysis of the forced response of mistuned cyclic assemblies". *AIAA Journal*, **28**(5), May, pp. 861–868.
- [18] Liao, H., Wang, J., Yao, J., and Li, Q., 2010. "Mistuning forced response characteristics analysis of mistuned bladed disks". *Journal of Engineering for Gas Turbines and Power*, **132**(12), December, pp. 122501.1–122501.11.
- [19] Avalos, J., Mignolet, M. P., and Soize, C., 2009. "Response of bladed disks with mistuned blade-disk interfaces". *Proceedings of ASME Turbo Expo 2009: Power for Land, Sea and Air*(ASME Paper GT2009-59580), June 8-12.
- [20] Petrov, E. P., and Ewins, D. J., 2003. "Analysis of the worst mistuning patterns in bladed disk assemblies". *Journal of Turbomachinery*, **125**(4), October, pp. 623–631.

- [21] Lin, C. C., and Mignolet, M. P., 1996. “Effects of damping and damping mistuning on the forced vibration response of bladed disks”. *Journal of Sound and Vibration*, **193**(2), pp. 525–543.
- [22] Han, Y., Xiao, B., and Mignolet, M. P., 2007. “Expedient estimation of the maximum amplification factor in damped mistuned bladed disks”. *Proceedings of GT2007 ASME Turbo Expo 2007: Power for Land, Sea and Air*(5), May 14–17.
- [23] Berthillier, M., Dupont, C., Mondale, R., and Barrau, J. J., 1998. “Blades forced response analysis with friction dampers”. *Journal of Vibration and Acoustics*, **120**(2), April, pp. 468–474.
- [24] Griffin, J. H., and Sinha, A., 1985. “The interaction between mistuning and friction in the forced response of bladed disk assemblies”. *Journal of Engineering for Gas Turbines and Power*, **107**(1), January, pp. 205–211.
- [25] Wei, S. T., and Pierre, C., 1989. “Effects of dry friction damping on the occurrence of localized forced vibrations in nearly cyclic structures”. *Journal of Sound and Vibration*, **129**(3), pp. 397–416.
- [26] Yoo, H. H., Kim, J. Y., and Inman, D. J., 2003. “Vibration localization of simplified mistuned cyclic structures undertaking external harmonic force”. *Journal of Sound and Vibration*, **261**(5), pp. 859–870.
- [27] Turcotte, J. S., Hollkamp, J. J., and Gordon, R. W., 1998. “Vibration of a mistuned bladed-disk assembly using structurally damped beams”. *AIAA Journal*, **36**(12), December, pp. 2225–2228.
- [28] Krzyzynski, T., Popp, K., and Sestro, W., 2000. “On some regularities in dynamic response of cyclic periodic structures”. *Chaos, Solitons and Fractals*, **11**(10), pp. 1597–1609.
- [29] Ewins, D. J., 1973. “Vibration characteristics of bladed disc assemblies”. *Journal of Mechanical Engineering Science*, **2**(5), pp. 165–186.
- [30] Afolabi, D. H., 1982. “Vibration of mistuned bladed disc assemblies”. Phd thesis, University of London, London, UK.
- [31] Petrov, E. P., 2008. “Explicit finite element models of friction dampers in forced response analysis of bladed disks”. *Journal of Engineering for Gas Turbines and Power*, **130**, March, pp. 022502.1–022502.11.
- [32] Feiner, D. M., and Griffin, J. H., 2002. “A fundamental model of mistuning for a single family of modes”. *Journal of Turbomachinery*, **124**(4), October, pp. 597–605.
- [33] Feiner, D. M., and Griffin, J. H., 2004. “Mistuning identification of bladed disks using a fundamental mistuning model - part 1: Theory”. *Journal of Turbomachinery*, **126**(1), pp. 150–158.
- [34] Siewert, C., and Stuer, H., 2010. “Forced response analysis of mistuned turbine bladings”. *Proceedings of ASME Turbo Expo 2010: Power for Land, Sea and Air*, **6**, June.
- [35] Petrov, E. P., Santilurk, K. Y., and Ewins, D. J., 2002. “A new method for dynamic analysis of mistuned bladed disks based on the exact relationship between tuned and mistuned systems”. *Journal of Engineering for Gas Turbines and Power*, **124**(3), July, pp. 586–597.
- [36] Hart, G. C., 1996. “Random damping in buildings”. *Journal of Wind Engineering and Industrial Aerodynamics*, **59**(2-3), March, pp. 233–246.
- [37] Kareem, A., and Sun, W. J., 1990. “Dynamic response of structures with uncertain damping”. *Journal of Wind Engineering and Industrial Aerodynamics*, **12**(1), January, pp. 2–8.
- [38] Kareem, A., and Gurley, K., 1996. “Damping in structures: its evaluation and treatment of uncertainty”. *Journal of Wind Engineering and Industrial Aerodynamics*, **59**(2-3), March, pp. 131–157.
- [39] Bishop, R. E. D., 1958. “On damped free vibration with particular reference to systems having nearly equal natural frequencies”. *The Aeronautical Quarterly*, **9**, February, pp. 71–95.
- [40] Lim, S., Bladh, R., Castanier, M. P., and Pierre, C., 2007. “A compact, generalized component mode mistuning representation for modeling bladed disk vibration”. *AIAA Journal*, **45**(9), pp. 2285–2298.
- [41] Craig, R. R., 1981. *Structural Dynamics, An Introduction to Computer Methods*. John Wiley and Sons, New York.
- [42] Bampton, C. R., 1968. “Coupling of substructures for dynamics analysis”. *AIAA Journal*, **6**(7), pp. 1313–1319.
- [43] Craig, R. R., and Chang, C. J., 1976. “Free-interface methods of substructure coupling for dynamic analysis”. *AIAA Journal*, **14**(11), November, pp. 1633–1635.
- [44] Yang, M. T., and Griffin, J. H., 2001. “A reduced-order model of mistuning using a subset of nominal system modes”. *ASME Journal of Engineering for Gas Turbines and Power*, **123**(4), October, pp. 893–900.
- [45] Yang, M. T., and Griffin, J. H., 1997. “A normalized modal eigenvalue approach for resolving modal interaction”. *ASME Journal of Engineering for Gas Turbines and Power*, **119**(3), July, pp. 647–650.
- [46] Castanier, M. P., and Pierre, C., 2006. “Modeling and analysis of mistuned blade disk vibration: Status and emerging directions”. *Journal of Propulsion and Power*, **22**(2), March–April, pp. 384–396.